

# Kinematics of the Outer Stellar Halo

Chris Flynn<sup>1,2</sup>, J. Sommer-Larsen<sup>3</sup> & P. R. Christensen<sup>3,4</sup>

<sup>1</sup>NORDITA,  
Blegdamsvej 17, DK-2100 Copenhagen Ø, Denmark

<sup>2</sup>Tuorla Observatory,  
Väisäläntie 20, FIN-21500 Piikkiö, Finland

<sup>3</sup>Theoretical Astrophysics Center,  
Blegdamsvej 17, DK-2100 Copenhagen Ø, Denmark

<sup>4</sup>The Niels Bohr Institute,  
Blegdamsvej 17, DK-2100 Copenhagen Ø, Denmark

## Summary

We have tested whether the simple model for the kinematics of the Galactic stellar halo (in particular the outer halo) proposed by Sommer-Larsen, Flynn and Christensen (SLFC) is physically realizable, by directly integrating particles in a 3-D model of the Galactic potential. We are able to show that the SLFC solution can be realized in terms of a distribution of particles with stationary statistical properties in phase-space. Hence, the SLFC model, which shows a notable change in the anisotropy from markedly radial at the sun to markedly tangential beyond about Galactocentric radius  $r = 20$  kpc, seems a tenable description of outer halo kinematics.

# 1 Introduction

In recent years various techniques have been developed to isolate field halo stars in situ, so that increasingly, samples of these stars are becoming available with which to address questions about the kinematic structure of the halo. Radial velocity and distance measurements of these objects provide important constraints on models of the kinematics and more indirectly the distribution of the dark matter in which the visible galaxy is apparently embedded.

Flynn, Sommer-Larsen and Christensen (1994) have developed techniques using broadband photoelectric photometry and medium dispersion spectroscopy for isolating Blue Horizontal Branch (BHB) stars in the outer Galactic halo and have assembled a catalog in four fields of about 100 stars with line-of-sight velocities and distances (Flynn et. al. 1995). Sommer-Larsen, Flynn and Christensen (1994, hereafter SLFC) developed a model of the kinematics of the outer halo, which fits the observations surprisingly well, given the simple nature of the model. They assumed that the outer stellar halo is a round, non-rotating system with a density falloff with Galactocentric radius like  $r^{-3.4}$  and that the Galactic rotation curve is flat to large Galactic radii ( $r \gg R_\odot$ ) where  $R_\odot$  is the sun's distance from the Galactic center. The Jeans equation was then solved for the radial and one-dimensional tangential velocity dispersions ( $\sigma_r, \sigma_t$ ) as functions of  $r$  by fitting the observed line-of-sight velocity dispersions as a function of line-of-sight distance.

Their results indicate that the halo kinematics in the outer halo are *tangentially* anisotropic, whereas they are *radially* anisotropic near the sun. Specifically, near the sun,  $\sigma_r \approx 140 \text{ km s}^{-1}$  and  $\sigma_t \approx 90\text{-}100 \text{ km s}^{-1}$ , whereas SLFC find a major kinematic change in the outer halo ( $r \gtrsim 10 - 20$ ) kpc, where  $\sigma_r \approx 80 - 100 \text{ km s}^{-1}$  and  $\sigma_t \approx 130\text{-}150 \text{ km s}^{-1}$ .

The solution to the Jeans equation only provides the second moments of the velocity distribution in the halo. To demonstrate that the solution for ( $\sigma_r, \sigma_t$ ) is actually physical, one must show that the velocity dispersions can be realized in terms of a stationary phase-space distribution function  $f$  which is everywhere non-negative in phase-space. Although there are methods in the literature for recovering the distribution function from simple potential-density pairs and the velocity dispersions (see Binney and Tremaine (1987) pp255 and references therein), the extension of these methods to the case of the Galactic potential is a formidable analytic task. Since we would nevertheless like to test that the SLFC model is physical, we have taken in this paper a less ambitious and more direct approach: we place a large number of test particles with the kinematic characteristics of the SLFC type model (using a simple assumption about their velocity distribution) into a realistic 3-dimensional model of the Galaxy's potential, and integrate the orbits over a Hubble time, allowing the system to phase mix. We show in this way that a stationary system can be realized with the kinematic and spatial properties of the SLFC model.

In section 2 we develop a realistic model of the Galactic potential. In section 3 we describe our simulations of the SLFC kinematics, and we discuss the results and draw conclusions in section 4.

## 2 A Galactic Potential

We have developed a multi-component model of the Galactic potential which we have matched with good accuracy to Galactic parameters, such as the rotation

curve, local disk density and disk scale length.

The Galactic potential  $\Phi(R, z)$  is modeled in cylindrical coordinates where  $R$  is the planar Galactocentric-radius and  $z$  is the distance above the plane of the disk. The total potential  $\Phi$  is modeled by the sum of the potentials of the dark halo  $\Phi_H$ , a central component  $\Phi_C$  and disk  $\Phi_D$ :

$$\Phi = \Phi_H + \Phi_C + \Phi_D.$$

The potential of the dark halo  $\Phi_H$  is assumed to be spherical and of the form

$$\Phi_H = \frac{1}{2} V_H^2 \ln(r^2 + r_0^2)$$

where  $r$  is the Galactocentric radius ( $r^2 = R^2 + z^2$ ). The potential has a core radius  $r_0$  and  $V_H$  is the circular velocity at large  $r$  (i.e. relative to the core radius).

The potential of the central component  $\Phi_C$  is modeled by two spherical components, representing the bulge/stellar-halo and an inner core component:

$$\Phi_C = -\frac{GM_{C_1}}{\sqrt{r^2 + r_{C_1}^2}} - \frac{GM_{C_2}}{\sqrt{r^2 + r_{C_2}^2}}.$$

Here  $G$  is the gravitational constant,  $M_{C_1}$  and  $R_{C_1}$  are the mass and core radius of the bulge/stellar-halo term and  $M_{C_2}$  and  $R_{C_2}$  are the mass and core radius of the inner core.

The disk potential  $\Phi_D$  is modeled using an analytical form which is a combination of three Miyamoto-Nagai potentials (Miyamoto and Nagai 1975)

$$\Phi_D = \Phi_{D_1} + \Phi_{D_2} + \Phi_{D_3}.$$

where

$$\Phi_{D_n} = \frac{-GM_{D_n}}{\sqrt{(R^2 + (a_n + \sqrt{(z^2 + b^2)})^2)}} \quad n = 1, 2, 3$$

Here the parameter  $b$  is related to the disk scale height,  $a_n$  to the disk scale length and  $M_{D_n}$  are the masses of the three disk components. Adopting a single Miyamoto-Nagai potential for the disk and reasonable dark halo potentials leads to the problem that the disk scale length is too short (typically by a factor of 2) for well fitting rotation curves. We have circumvented this difficulty by combining three Miyamoto-Nagai disks of differing scale lengths and masses (the parameters for which are shown in Table 1). The parameters have essentially been chosen to be consistent with the dynamical mass measurements of the disk surface density at the solar circle, while maintaining a good fit to the rotation curve and a realistic disk scale length. Note particularly that for the  $n = 2$  component the mass  $M_2$  is negative. The densities resulting from the disk potential alone, as well as the total potential, are nevertheless positive everywhere.

The rotation curve of our model is shown in Figure 1, together with the contributions from the various components. Assuming  $R_\odot = 8$  kpc, the local disk surface density of matter  $\Sigma_{\text{Disk}}(R = R_\odot)$  is  $51 M_\odot \text{pc}^{-2}$ , consistent with recent dynamical measurements which measure about  $50 M_\odot \text{pc}^{-2}$  (Kuijken and Gilmore 1989, Flynn and Fuchs 1994). The local midplane density of the disk (i.e at  $R = R_\odot$ ) is  $0.09 M_\odot \text{pc}^{-3}$ . The surface density  $\Sigma_{\text{Disk}}$  is plotted as a function of  $R$

Component	Parameter	Value
Dark Halo	$r_0$	8.5 kpc
	$V_H$	220 km s <sup>-1</sup>
Bulge/Stellar-halo	$r_{C_1}$	2.7 kpc
	$M_{C_1}$	$3.0 \times 10^9 M_\odot$
Central comp.	$r_{C_2}$	0.42 kpc
	$M_{C_2}$	$1.6 \times 10^{10} M_\odot$
Disk	$b$	0.3 kpc
	$M_{D_1}$	$6.6 \times 10^{10} M_\odot$
	$a_1$	5.81 kpc
	$M_{D_2}$	$-2.9 \times 10^{10} M_\odot$
	$a_2$	17.43 kpc
	$M_{D_3}$	$3.3 \times 10^9 M_\odot$
	$a_3$	34.86 kpc

Table 1: Adopted Parameters for the Galactic Potential

in Figure 2, and the disk is seen to be exponential over a large range in  $R$ ; it has a scale length of 4.1 kpc, in good agreement with observation (see e.g. Lewis and Freeman 1989 and references therein). The disk has a uniform scale height with  $R$  of about 260 pc.

### 3 Numerical Methods

SLFC obtained a best fit solution for the second moments of the radial and tangential velocity distributions of the stellar halo for  $r \geq R_\odot$ . We now describe our simulations in the potential described above, and show there is a strong indication that the SLFC model is physically realizable.

We started by testing whether a phase-space distribution function with a Gaussian velocity distribution and second velocity moments given by the SLFC model is stationary in our model potential, i.e. the phase-space distribution function does not depend explicitly on time. We set up  $5 \times 10^4$  tracer particles in the potential described above, with a density distribution falling like  $r^{-3.4}$ , truncated inside 0.1 kpc and outside 200 kpc. Initial particle velocities were randomly drawn from Gaussian distributions with radial and tangential velocity dispersions  $\sigma_r(r)$  and  $\sigma_t(r)$  as specified by the SLFC (from their equations 3 and 4; see also their Figure 2). The orbits of the particles were integrated using a Runge-Kutta scheme with an adaptive step size (Press et. al. 1992) over a period of 15 Gyr, and the density and velocity dispersions of the particles as functions of  $r$  were determined at 1 Gyr intervals. The results of the calculations are shown at 5 Gyr intervals in Figure 3. Initially, the particles (Panels (a) and (b)) have velocity dispersions and density falloff corresponding exactly (within the statistical errors) to the SLFC model. The evolution of the density and velocity dispersions is shown over the 15 Gyr in panels (c)—(h). The velocity dispersions changed quickly (in less than a Gyr), and the test ensemble reaches a stationary phase-mixed state in which the

Figure 1

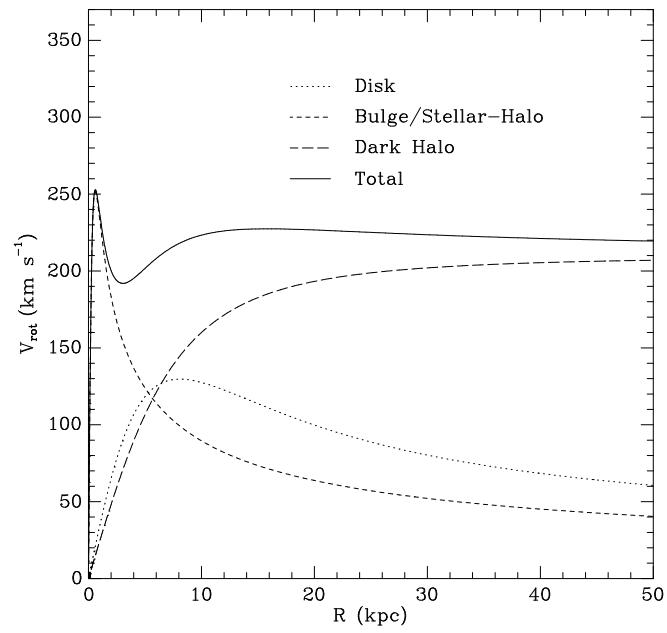


Figure 1: The rotation curve of our model galaxy. The solid line is the total rotation curve, the other lines indicate the partial contributions to the rotation curve by the three components.

Figure 2

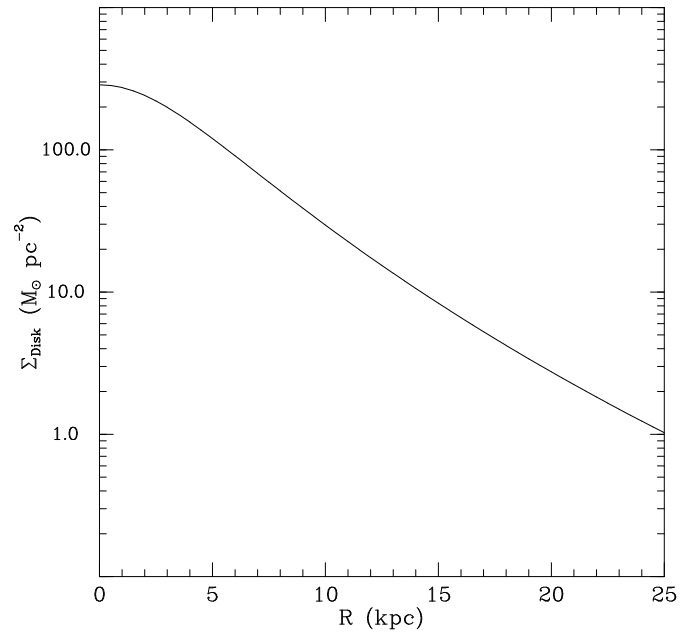


Figure 2: Surface density  $\Sigma_{\text{Disk}}$  in  $M_{\odot} \text{pc}^{-2}$  of the disk component of the model potential as a function of radius in the plane,  $R$ . This density falloff is close to an exponential with scale length of 4.1 kpc.

velocity distribution has become everywhere more isotropic relative to the initial conditions. The density falloff is very insensitive to these changes, remaining virtually unchanged and well fitted by a  $r^{-3.4}$  power-law (indicated by the lines in panels (d), (f) and (h)) during the entire simulation.

Motivated by this decrease of the velocity anisotropy with time, we performed the following experiment: we increased the initial velocity anisotropy as a function of  $r$ , by replacing the SLFC parameters  $\sigma_o^2$  and  $\sigma_+^2$  by the primed quantities  $\sigma'_o{}^2$  and  $\sigma'_+{}^2$ . (These parameters characterize the radial velocity variances in the inner and outer halo model; see SLFC's eqs (3) and (4) and SLFC Figure 2).

$$\sigma'_+{}^2 = \lambda\sigma_+^2, \quad \lambda \geq 1$$

and

$$\sigma'_o{}^2 = \sigma_o^2 + \frac{1}{2}(1.0 - \lambda)\sigma_+^2 \quad \lambda \geq 1$$

The effect of this transformation is best seen by looking at the dotted line in Figure 4(a) (for the case  $\lambda = 1.6$ ) — the velocity anisotropy is increased in the inner and outer regions of the halo, relative to the SLFC model. We then performed the simulations again, for different values of  $\lambda$ , corresponding to different initial conditions.

This simple strategy yielded quite satisfactory results. In particular, we show in Figure 4 for the most satisfactory case,  $\lambda = 1.6$ , the evolution of  $\sigma_r$ ,  $\sigma_t$  and density over 15 Gyr. As before, the velocities evolve quickly ( $< 1$  Gyr) to a more isotropic state, becoming a good match to the SLFC model. The density falloff remains virtually unaffected as before, and remains a good fit to the  $r^{-3.4}$  power law.

Two further physical properties of the simulation were examined. In the SLFC model, we assumed for simplicity that firstly, the density falloff of the halo is spherically symmetric, and secondly, that the two azimuthal velocity dispersions (in radial coordinates,  $\sigma_\phi$  and  $\sigma_\theta$ ) were equal (and denoted by  $\sigma_t$ ). In the simulation, the initial state was given these properties, but since the integrations were fully three-dimensional, these properties were free to evolve with time. In order to check the self consistency of the stationary phase-mixed result of the simulation with the SLFC model, we examined both these properties as functions of time.

Firstly, Figure 5 shows the density contours of the particles in the  $(x, z)$ -plane, after they have attained their stationary configuration. Hartwick (1984), using samples of RR Lyrae stars in many directions, has shown that while the outer halo (here taken as  $r \gtrsim 10 - 20$  kpc) is close to being spherically symmetric, the inner halo may be quite flattened, and in fact Larsen and Humphries (1994) have recently argued that the inner halo may be flattened by as much as 2 to 1. In this paper however, we are primarily concerned with the behaviour of the outer halo, where the SLFC model is constrained by observations. Figure 5 shows that the outer halo (i.e  $r \gtrsim 10 - 20$  kpc) does remain spherically symmetric in the simulation, consistent with the SLFC assumption, but that the inner halo (particularly inside the solar circle) has been somewhat flattened in response to the potential, though not as much as Larsen and Humphries propose. We do stress however, that the SLFC model primarily meant to describe the outer halo (and is constrained by observations in the outer halo only), so the behaviour of the simulation in the inner halo must be regarded with due caution.

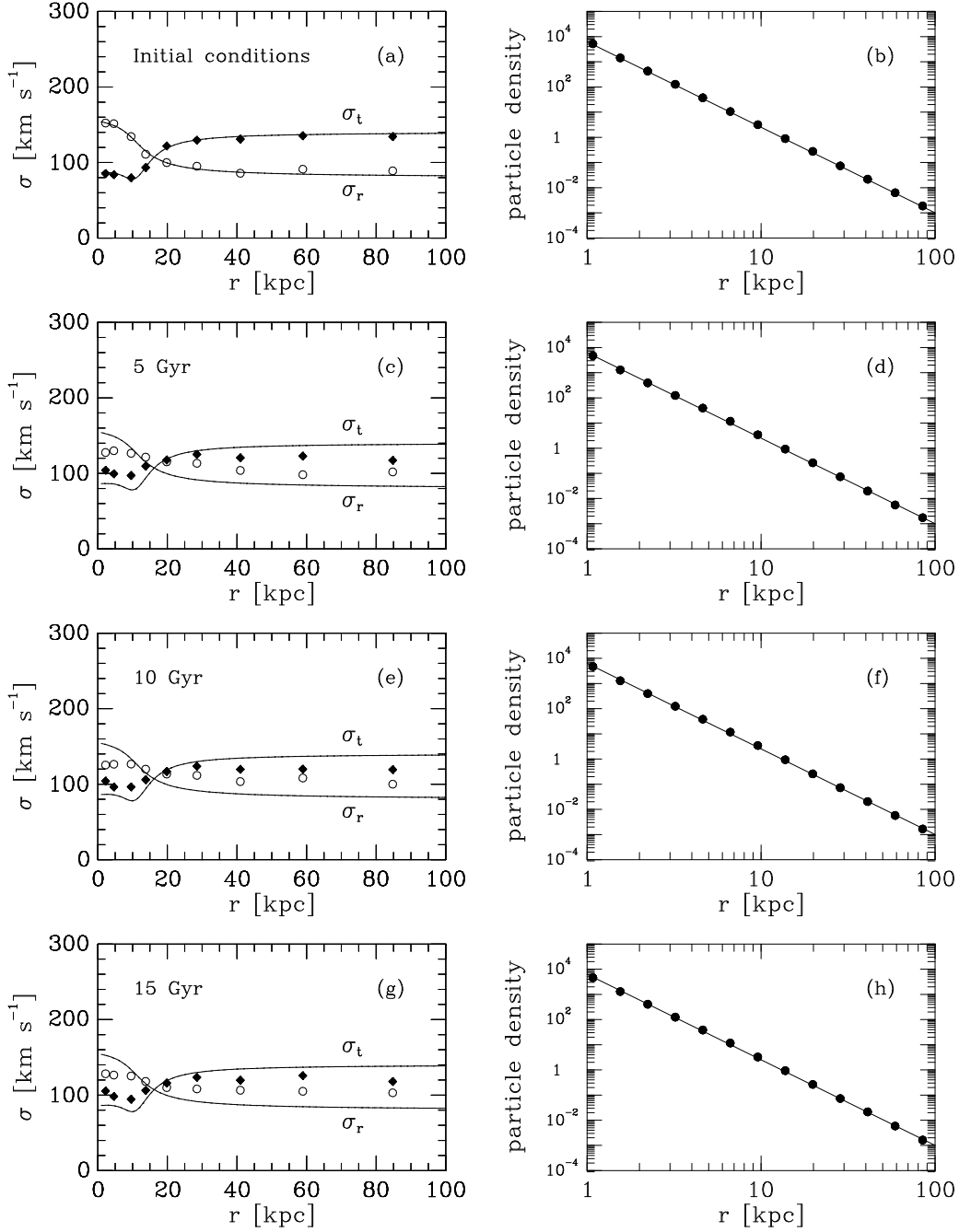


Figure 3: The response of the particles to the potential as a function of time is shown by their radial and tangential velocity dispersions,  $\sigma_r$  and  $\sigma_t$  (lefthand panels) and by their number density ( $\text{kpc}^{-3}$ ) (righthand panels), both as functions of Galactocentric radius  $r$ . The particles initially have  $\sigma_r$  (open symbols) and  $\sigma_t$  (solid symbols) as specified by the SLFC model (indicated by solid lines), and the random velocities of the particles are initially Gaussian. The system relaxes quickly to a more isotropic state.



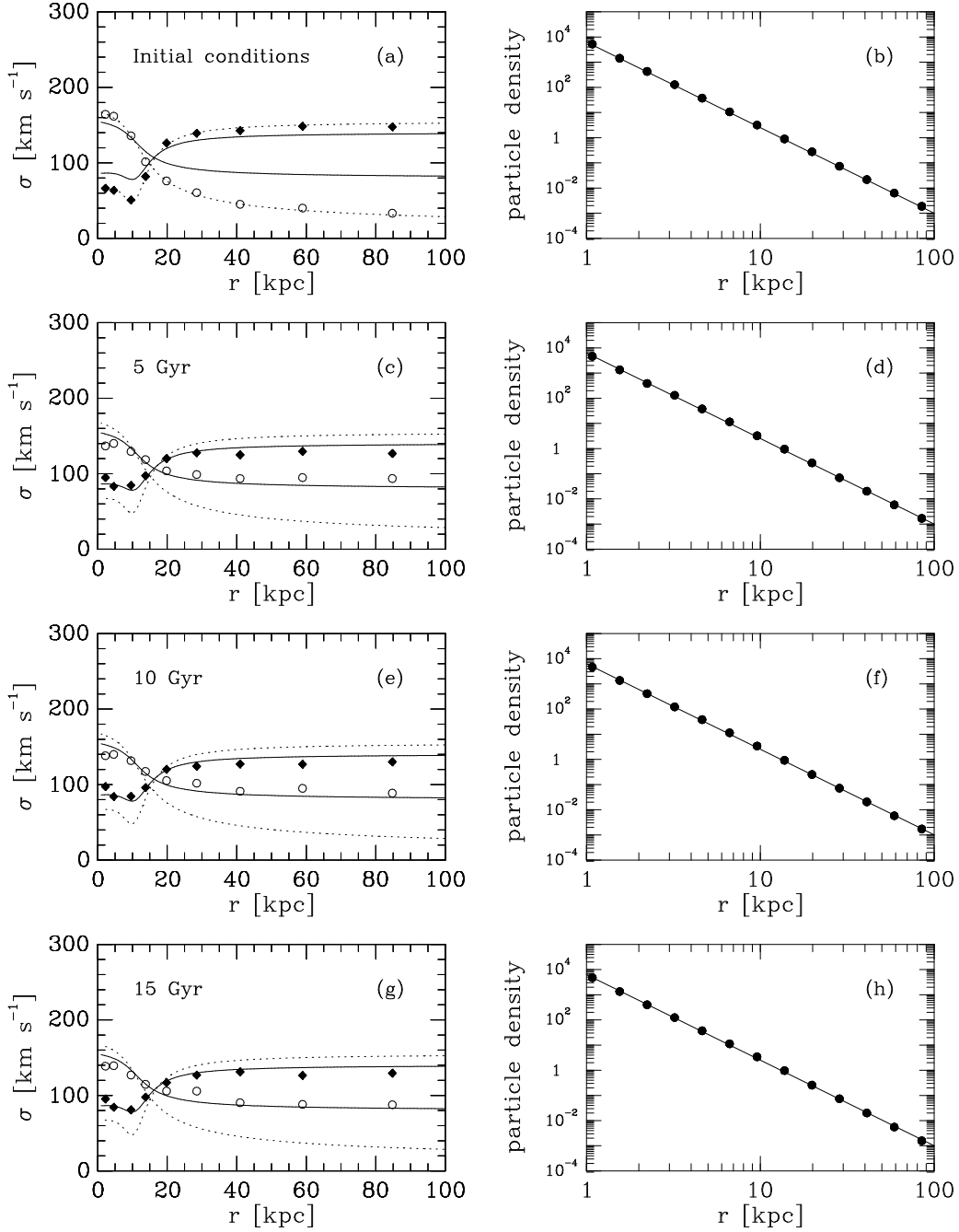


Figure 4: Symbols are as for Figure 3. Here, the initial anisotropy of the system has been artificially enhanced as is described in section 3, and as indicated by the dashed lines. The particles relax quickly and become a quite good stationary fit to the SLFC model (shown by solid lines). This procedure strongly indicates that a stationary system, having the characteristics of the SLFC model, can exist.

Figure 5

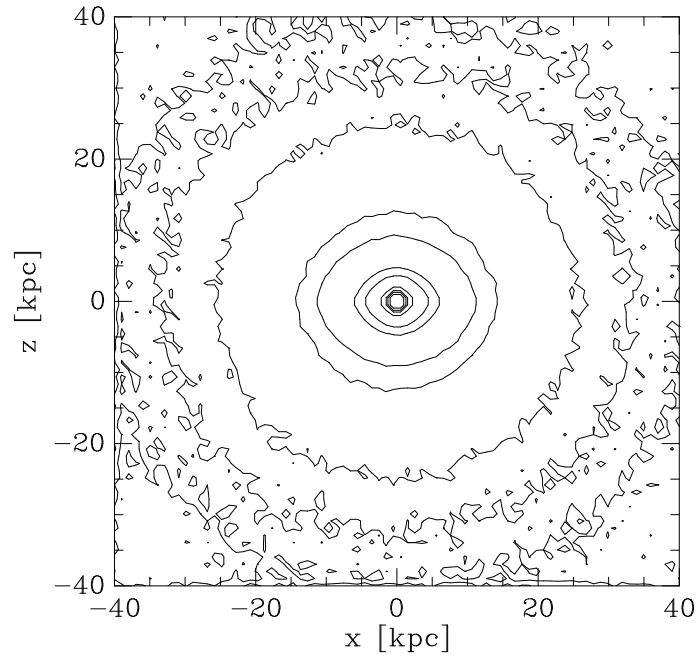


Figure 5: The density distribution of the particles in the simulation in Figure 4, shown in the  $(x, z)$ -plane, after the model reaches its stationary state. The initial state of the simulation was spherically symmetric. The outer parts of the simulation are still spherical, while the inner part has flattened somewhat in response to the potential.

Fig 6

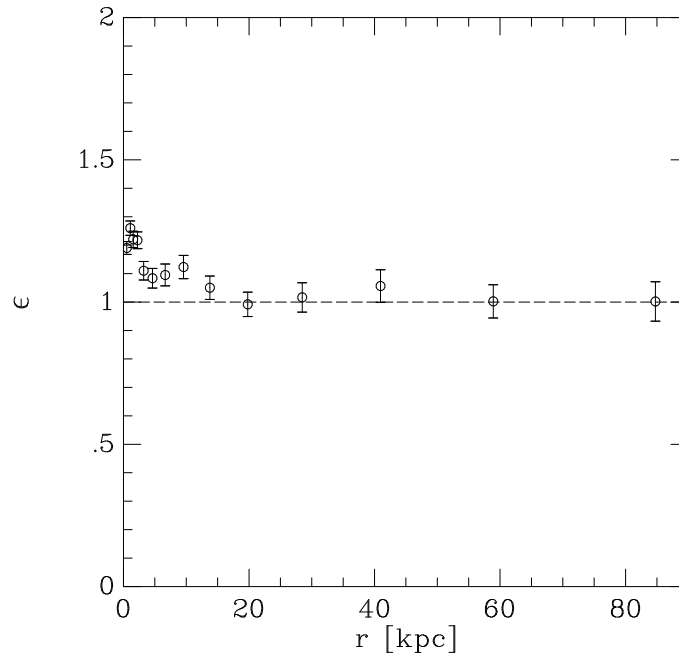


Figure 6: The ratio  $\epsilon = \sigma_\theta / \sigma_\phi$  as a function of Galactocentric radius,  $r$ , after the simulation reaches its stationary state. The SLFC model assumes that  $\epsilon = 1.0$  in the outer halo, and the simulation matches this well.

Secondly, we examined the ratio  $\epsilon = \sigma_\theta/\sigma_\phi$  which is shown as a function of Galactocentric radius  $r$  in Figure 6, again plotted after the model has attained a stationary state. By assumption  $\epsilon = 1$  initially, but is free to evolve in the simulation. As with the density distribution, the inner and outer regions responded differently. In the outer halo,  $\epsilon$  remains a good fit to the SLFC assumption of  $\epsilon = 1.0$ , whereas  $\epsilon$  departs slightly from this value in the inner halo. We stress again that the SLFC data only constrain the behaviour of the outer halo, and it is only in the outer halo that we require that  $\epsilon$  should be consistent with the SLFC model.

In all the discussed simulations, the particles are kinematically reorganized, arriving rapidly at a stationary state. The response in each case is primarily in the velocity distribution of the particles, which evolves away from its initially Gaussian form, while the overall density falloff with Galactocentric radius is hardly affected, although some flattening occurs in the inner halo. If the particles start with Gaussian velocity distribution with second moments exactly matching the SLFC model, then the kinematic reorganization leads to a stationary state which is no longer a match to the SLFC model. However, for  $\lambda = 1.6$  the initially Gaussian velocity distribution reorganizes itself into a new distribution which is a close and stationary match to the SLFC model. This shows that at least one velocity distribution exists with second moments matching the SLFC model, and which remains stationary in the adopted potential. Hence we have a strong indication that the solutions of the SLFC model for the velocity dispersions in the outer halo can be realized physically.

## 4 Discussion and Conclusions

We have tested the simple model for the kinematics of the Galactic halo (in particular the outer halo) proposed by SLFC, by directly integrating particles in a realistic 3-D model of the Galactic potential, under the assumption of an initially Gaussian velocity distribution. We found that the particles relax somewhat into the potential with time, the kinematics becoming everywhere more isotropic. We experimented with models where we increased the initial anisotropy compared to the SLFC model, and found a configuration which after a short relaxation period ( $\approx 1$  Gyr) becomes a quite good and stationary fit to the SLFC model. Hence, the SLFC model, which shows a notable change in the velocity anisotropy from markedly radial at the sun to markedly tangential beyond about  $r = 20$  kpc, seems a tenable description of outer halo kinematics.

The origin of the change in the anisotropy with Galactocentric radius remains unclear. We are currently gathering further data in the outer halo at the poles and in the anti-center directions to test the model more directly. We are also currently involved in a series of hydrodynamical and N-body simulations of disk galaxy formation including star-formation in which the kinematics of successive generations of stars can be examined, and we expect the observed variation in the velocity anisotropy with  $r$  of the halo to be an interesting constraint on the simulations.

## Acknowledgments

We would like to thank Burkhard Fuchs for helpful discussions. CF is very grateful to the Alexander von Humboldt Foundation (Bonn) for funding and for the hospitality at the Astronomisches Rechen-Institut in Heidelberg, where part of this research was carried out. This work was supported in part by Danmarks Grundforskningsfond through its support of the Theoretical Astrophysics Center.

## References

- Binney, J. and Tremaine, S. 1987. in *Galactic Dynamics*, Princeton University Press, Princeton, New Jersey.
- Flynn, C. and Fuchs, B. 1994, MNRAS, 270, 471.
- Flynn, C., Sommer-Larsen, J. and Christensen, P.R. 1994, MNRAS, 267, 77.
- Flynn, C., Sommer-Larsen, J., Christensen, P.R. and Hawkins, M.R.S., 1995, A&ASupp, 109, 171.
- Hartwick, F.D.A. 1987, in *The Galaxy: (Reidel, Dordrecht)*p. 281
- Kuijken, K and Gilmore, G. 1989, MNRAS, 239, 651.
- Larsen, J.A. and Humphries, R.M., 1994, ApJL, 436, L149.
- Lewis, J. and Freeman, K.C., 1989, AJ, 97, 139.
- Miyamoto, M. and Nagai, R., 1975, Pub. Ast. Soc. Jap. 27, 533.
- Press, W.H., Flannery, B.P., Teukolsky, S.A. and Vetterling, W.T. 1986, *Numerical Recipes*.
- Sommer-Larsen, J., Flynn C. and Christensen, P.R. 1994, MNRAS, 271, 94.